Spatial variation in potential and realized growth of juvenile Pacific cod in the southeastern Bering Sea

Thomas P. Hurst[1,*], Jessica A. Miller[2], Nissa Ferm[3], Ron A. Heintz[4], Edward V. Farley[4]

[1]Fisheries Behavioral Ecology Program, Resource Assessment and Conservation Engineering Division,
Alaska Fisheries Science Center, National Marine Fisheries Service, National Oceanic and Atmospheric Administration,
Hatfield Marine Science Center, Newport, OR 97165, USA

[2]Department of Fisheries and Wildlife, Coastal Oregon Marine Experiment Station, Hatfield Marine Science Center,
Oregon State University, 2030 SE Marine Science Drive, Newport, OR 97365, USA

[3]Recruitment Processes Program, Resource Assessment and Conservation Engineering Division,
Alaska Fisheries Science Center, National Marine Fisheries Service, National Oceanic and Atmospheric Administration, 7600
Sand Point Way NE, Seattle, WA 98115, USA

[4]Auke Bay Laboratories, Alaska Fisheries Science Center, National Marine Fisheries Service,
National Oceanic and Atmospheric Administration, 17109 Point Lena Loop Road, Juneau, AK 99801, USA

ABSTRACT: In the southeast Bering Sea, age-0 Pacific cod *Gadus macrocephalus* primarily occupy 2 distinct habitat types: shallow, coastal waters along the central Alaska Peninsula and surface waters over the broad continental shelf. We examined functional aspects of habitat use by describing regional and habitat-specific variation in feeding and growth energetics based on sampling conducted in late summer 2012. Diets varied among regions, with more benthic copepods, amphipods, and shrimps consumed in coastal regions and more pelagic copepods, krill, and pteropods consumed in surface waters over the shelf. Growth rates measured from otolith edge increments were highest along the Alaska Peninsula, the region supporting the highest density of age-0 cod. Interestingly, fish energetic condition was comparatively low in the region with the highest growth rates, suggesting a tradeoff between growth and energy storage. Water temperatures and prey energy densities were used with a bioenergetic model to derive spatially explicit estimates of growth potential. Growth potential was correlated with observed station-specific growth rates, providing an independent, empirical validation of the model. We also contrasted patterns of growth potential in 2012, a cold year in the Bering Sea, with those for 2005, a representative warm year. Growth potential was reduced in the warm year by up to 27 %, and there was a shift in the region offering the highest growth potential. The observed thermally induced changes in growth potential, as well as the location of highest growth potential, may have significant implications for the recruitment of this important resource species under episodic or prolonged warming.

KEY WORDS: Bering Sea · Growth rate · Bioenergetics · Nursery habitat · Diet

INTRODUCTION

The southeast Bering Sea (SEBS) shelf supports important fisheries for gadids, including Pacific cod *Gadus macrocephalus*, walleye pollock *Gadus chalcogrammus*, and multiple species of crabs, salmon, and flatfishes. Understanding the distribution and habitat use patterns of these species is critical to their conservation and predicting the consequences of environmental and climate variation. Habitat use during the first year of life is particularly important because rates of growth and mortality are driven by the experienced biotic and abiotic conditions and have significant implications for the recruitment dynamics of the stock (Houde 1987, Pörtner & Peck 2010).

Recruitment of gadids in the Atlantic and Pacific oceans has been linked to environmental conditions that directly influence growth capacity as well as the distribution and abundance of critical prey species during the first summer of life (e.g. Beaugrand & Kirby 2010, Stige et al. 2015, Sigler et al. 2016). Cold years in the North Sea and Bering Sea favor the production of large-bodied copepods which are beneficial to the growth and survival of larval and juvenile gadids (Beaugrand & Kirby 2010, Coyle et al. 2011). In contrast, beneficial foraging conditions in the Barents Sea are associated with warm, rather than cold, conditions (Sundby 2000). The size advantage obtained from encountering a favorable foraging environment during the early life stages has been linked to subsequent recruitment (Heintz et al. 2013, Stige et al. 2015). Compared to these congeners, much less is known about the ecology of Pacific cod in the Bering Sea, but similar dynamics may regulate recruitment. For example, interannual variation in age-0 Pacific cod diets and energetic condition have been linked with thermal variation and prey field dynamics (Farley et al. 2016), and the population has historically exhibited synchronous recruitment dynamics with co-occurring walleye pollock (Mueter et al. 2007).

Recent efforts using a variety of sampling approaches have improved our understanding of the dynamics of habitat use of Bering Sea cod (Parker-Stetter et al. 2013, Hurst et al. 2015, Miller et al. 2016). In the Bering Sea, age-0 cod use 2 distinct primary habitat types: coastal waters along the central Alaska Peninsula and surface waters over the broad continental shelf. The use of both coastal and offshore nursery habitats has also been recognized in Atlantic cod populations in Canada (Anderson & Dalley 1997, Dalley & Anderson 1997) and Norway (Bergstad et al. 1987, Salvanes et al. 2004). While important, these distributional studies represent only the first step in understanding habitat quality and the consequences of habitat variation. Improved understanding of the spatial variation in feeding and growth energetics of cod in the SEBS can identify linkages between spatial and temporal variation in habitat conditions and recruitment. Bioenergetic models offer a useful tool for integrating information on functional aspects of habitat use with the cumulative effects on growth potential reflecting spatial variation in habitat 'quality' (e.g. Benjamin et al. 2013). M. Zaleski et al. (unpubl. data) parameterized a bioenergetic model for age-0 cod to evaluate spatial variation in growth potential in the Gulf of Alaska. However, these analyses were focused on pelagic, shelf habitats and did not include coastal waters that

have been shown to be important habitats for juvenile cod in both the Gulf of Alaska and SEBS (Abookire et al. 2007, Laurel et al. 2007, Hurst et al. 2015).

In this study, we describe functional habitat use of age-0 Pacific cod in surface waters over the SEBS shelf and in coastal waters along the central Alaska Peninsula, the 2 habitats supporting the highest densities of age-0 cod (Hurst et al. 2015). Specifically, we describe spatial variation in diet composition, body size, and energetic condition. We also provide empirical evaluation of growth rate variation based on otolith increment analysis. This information was used with a bioenergetic model (M. Zaleski et al. unpubl. data) to describe spatial variation in growth potential in the SEBS. Regional variation in estimated growth potential was correlated with empirical estimates of growth rate, demonstrating the applicability of such model estimates. Finally, to illustrate the impacts of interannual variation in climate condition on the spatial variation in growth potential of juvenile Bering Sea cod, we compare spatial variation in growth potential in the study year of 2012 (a cold year) with those calculated in 2005 (a representative warm year).

MATERIALS AND METHODS

Fish collection

Large-scale patterns in physical and biological conditions in the Bering Sea are associated with latitudinal and depth gradients, resulting in recognized geographic zonation (see synthesis by Ortiz et al. 2016). The stratified middle shelf is separated from the well-mixed inner shelf by a persistent 'inner front' at ~50 m depth. A second, weaker front at ~100 m depth separates the middle shelf from the more weakly stratified outer shelf and slope (Kinder & Schumacher 1981, Overland et al. 1999). Offshore of the Alaska Peninsula, the inner front is generally weaker and closer to shore (~30 m; Cooper et al. 2014). Latitudinal patterns in daylight and sea ice retreat result in north–south differences in conditions which are most pronounced over the middle shelf (Ortiz et al. 2016). Based on these patterns (and consistent with Hurst et al. 2012, 2015), the sampling area of the SEBS was partitioned into 7 sampling regions for the analyses presented here (Fig. 1). The inner shelf was divided (clockwise) into Kuskokwim Bay (KB), Bristol Bay (BB), and the Alaska Peninsula (AKP). The middle shelf was separated into northern (NM) and southern (SM) regions, and the slope (SL) region included all waters deeper than 100 m. The Port
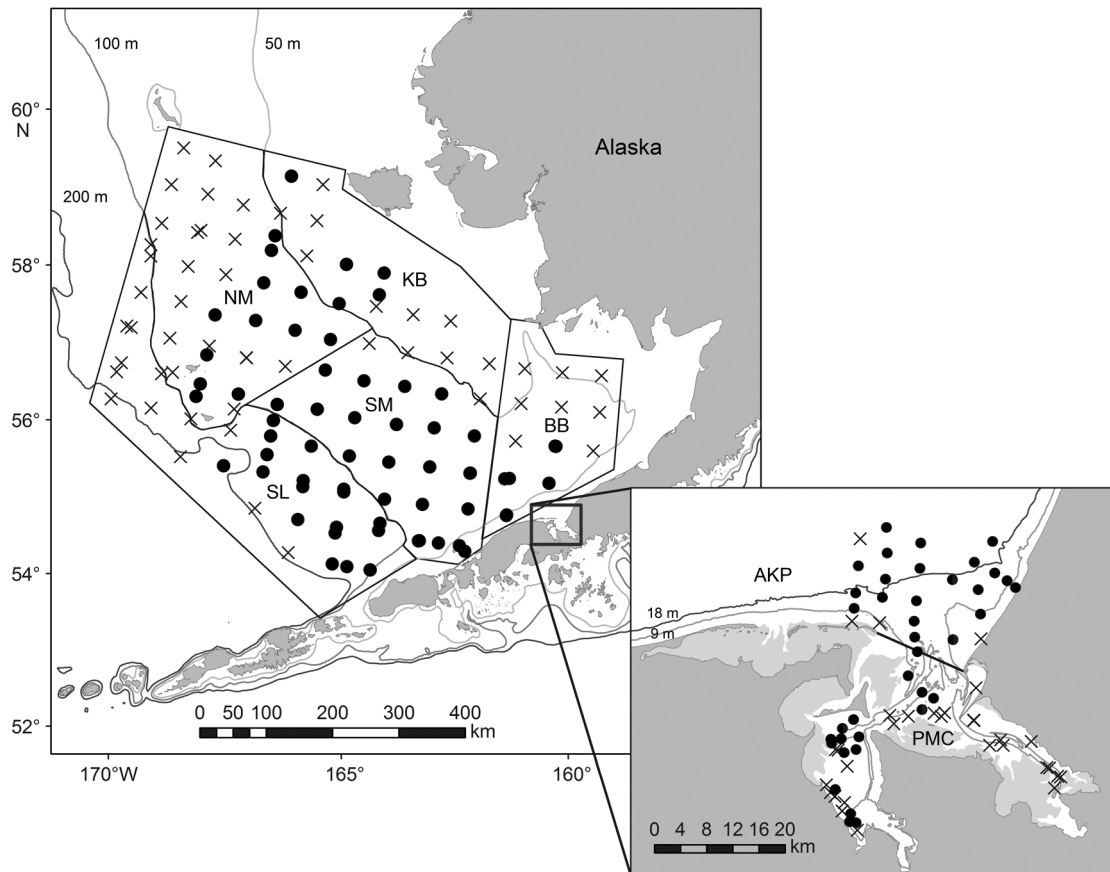
Fig. 1. Sampling stations for age-0 Pacific cod in the southeastern Bering Sea. ●: locations where age-0 cod were captured; '×' indicates a station was sampled, but no age-0 cod were captured. BB: Bristol Bay; KB: Kuskokwim Bay; SM: South Middle; NM: North Middle; SL: Slope; AKP: Alaska Peninsula; PMC: Port Moller Complex

Moller 'Complex' (PMC) included the coastal embayments of Port Moller and Herendeen Bay.

Fish used in this study were collected in synchronous sampling activities in the 2 primary habitat areas of age-0 Pacific cod in the Bering Sea in late summer 2012, with the number of sampled stations in each region ranging from 14 to 44 (Table 1). Fish in the shelf habitat regions (BB, KB, NM, SM, and SL) were collected with a 198 m midwater rope trawl. The net had a mouth opening of 55 m width × 15 m height

Table 1. Summary of sampling effort and biological sample sizes for age-0 Pacific cod in the southeastern Bering Sea by sampling region. Sampling effort was concentrated in the first half of the overall sampling interval, such that across regions most of the data was collected between 17 Aug and 15 Sep, 2012. This included 87% of trawls, 99% of fish lengths, 98% of diet samples, 99% of energy density measures, and 100% of otolith growth estimates. TL: total length; ED: energy density; GR: growth rate. See Fig. 1 for region abbreviations

Region	Sampling dates	Water depth range (m)	No. of tows	No. of TL measures (n tows)	No. of diet samples (n tows)	No. of ED samples (n tows)	No. of GR samples (n tows)
PMC	17–27 Aug	2–24	44	36 (16)	27 (14)	–	16 (9)
AKP	20–27 Aug	4–35	26	275 (21)	129 (19)	30 (3)	20 (2)
BB	20–23 Aug	37–75	15	65 (7)	27 (5)	19 (7)	4 (1)
SM	24 Aug–9 Sep	44–97	24	1077 (23)	131 (19)	67 (23)	26 (5)
KB	23 Aug–1 Oct	28–49	15	36 (6)	23 (5)	18 (6)	4 (1)
NM	17 Aug–15 Oct	49–99	32	135 (11)	16 (5)	25 (11)	5 (1)
SL	28 Aug–7 Oct	100–1195	32	609 (18)	79 (14)	48 (18)	21 (3)

with hexagonal mesh wings and a 1.2 cm mesh codend liner, and was towed for 30 min at 3.5 to 5 knots. Water temperatures were measured at 1 m depth from a CTD cast conducted prior to each tow for surface trawls and from a temperature sensor on the headrope of the net for midwater trawls. Sampling was conducted as per methods of Farley et al. (2007). Fish inhabiting the coastal habitat regions (AKP and PMC) were collected with a 3 m demersal beam trawl. The net had 7 mm mesh and a 4 mm mesh codend liner and was towed against the prevailing tidal current for 5 min. Following each tow, bottom water temperature was measured (YSI model 85) at the midpoint of the tow transect. Additional sampling details are presented in Hurst et al. (2015). Following collection, all age-0 cod were sorted from the catch and frozen for subsequent analyses. While the 2 different gears may have slightly different size-selectivities, this would have had only a minor effect on these results as we considered body size as a co-variate in most analyses and estimates of growth potential were calculated for a standardized size fish across the sampling region (see below).

Water temperature data measured during fish sampling were supplemented with the record of daily average temperature measured at 20 m depth at the M2 mooring site (56.78° N, 164.06° W) and output (K. Hedstrom & S. Danielson, Univ. Alaska-Fairbanks unpubl. data) from the Pan-Arctic Regional Oceanographic Modeling System (PAROMS) which encompasses the Bering Sea and Canadian Archipelago. PAROMS is a state-of-the-art, 3-dimensional, terrain-following, primitive equation model forced with sea ice, tides, and wind-driven circulation (based on Shchepetkin & McWilliams 2005). The model includes 50 variable-depth vertical layers with horizontal grid spacing of approximately 5 km in our study region.

Size and energetic condition

In the laboratory, all fish were thawed and measured (mm total length, TL). From each sample, 10 randomly selected fish (or all fish if catch < 10) were analyzed for condition factor, stomach fullness, and diet composition. In addition, fish from a subset of collection stations within each sampling region were analyzed for growth rate (GR, otolith increment widths) and energy density (ED). Wet weight condition (W_{dev}) was calculated as the deviation of each fish from the overall relationship between log-transformed TL and log-transformed wet weight (excluding stomach content weight).

A subsample of the collected cod was used to measure ED of fish in each region. Fish were analyzed according to Heintz et al. (2013). For most sampling stations, 3 fish were selected from those analyzed for diet composition. Stomach contents were removed and the remaining fish tissue was dried and homogenized. Equal amounts of tissue from the 3 fish were combined for analysis. Energy content was measured in a semi-micro bomb calorimeter (model 6725; Parr). In other cases, energetic content was measured on individual fish using the same procedures. Sample sizes ranged from 7 to 30 in each region (representing 19 to 60 fish), except for PMC where there were no additional fish available for energetic analyses.

Statistical analyses across sampling regions were performed with ANOVA with Tukey post hoc HSD tests. Where variances differed among sampling regions (as determined with Levene's test), non-parametric Kruskal-Wallace (K-W) ANOVA was performed with post hoc multiple comparisons. All analyses were performed with Statistica (v.6.1; Statsoft).

Diet analysis

Stomach content analysis was conducted on a total of 432 age-0 cod collected across 85 sampling locations. Stomachs were dissected from the fish and stored in 10% formalin for at least 30 d to fix tissues prior to identification of stomach contents. Stomach contents were weighed to 0.01 µg and stomach fullness expressed as the cumulative weight of stomach contents divided by fish wet mass (excluding stomach contents). Stomach contents were identified to the lowest practical taxonomic resolution (and developmental stage as appropriate). The number and total mass of each prey type were determined for each stomach. In addition to taxonomic diversity, we examined the functional diversity in cod diets. Each prey item and stage was assigned to a primary functional habitat category (endobenthic, epibenthic, hyperbenthic, drift, pelagic, and parasitic).

Diet composition was expressed as the mean percent weight (%W) and frequency of occurrence (%F) of each prey group within each sampling region. For the analyses presented here, prey types were aggregated into taxonomically homogeneous groups. ED_W values (kJ g^{-1} wet weight) were assigned to each prey type comprising at least 5% (mass) of the diet in any region (Table 2). Where available, we used values of ED_W measured for specific prey items collected in the Bering Sea. Where such values were unavail-

Table 2. Energetic content of prey items of age-0 Pacific cod in the southeast Bering Sea. Where available, estimates were based on published observations from the Bering Sea for specific taxa observed in the stomachs of Pacific cod captured during this study. AFSC: Alaska Fisheries Science Center

Prey type	Energy density (kJ g^{-1})	Sources
Amphipods (benthic)	2.95	Wilt (2012)
Amphipods (pelagic)	3.74	Davis et al. (1998), R. Heintz, AFSC unpubl. data, Whitman (2010)
Copepods (benthic)	4.71	R. Heintz, AFSC unpubl. data
Copepods (pelagic)	4.71	R. Heintz, AFSC unpubl. data
Shrimp (Carideans)	4.64	Perez (1990)
Crabs (zoea & megalopa)	2.98	Nishiyama (1977)
Cumaceans	3.37	Marrin Jarrin (2012)
Euphausiids	4.94	R. Heintz, AFSC unpubl. data, Whitman (2010)
Mysids	4.24	Perez (1990)
Pteropods	2.61	Davis et al. (1998)

able, we applied ED_W values of taxonomically related prey from other North Pacific waters. To estimate ED_W of cod diet at each station and sampling region, ED_W of each prey type was multiplied by the mean fraction (by mass) of that prey in the diet and summed across prey types. For each sampling region, mean prey energy density was multiplied by the mean gut fullness to estimate the total ED_W of stomach contents (expressed in J g^{-1} body weight of cod).

Variation in diet composition across sampling areas of the SEBS was described with nonmetric multidimensional scaling analysis (NMDS). Diet composition was averaged across all fish examined at each station. Stations with fewer than 5 diet samples were pooled with adjacent stations within the same sampling region for this analysis (resulting in n = 59 stations). Ordination was performed on a Bray-Curtis similarity matrix of arcsine-transformed diet composition (% of total mass). Patterns in diet composition were described by correlations of NMDS axes with habitat characteristics (temperature, water depth, latitude, and longitude) and biotic variables (fish length, condition, stomach fullness). NMDS analysis was performed with PC-ORD v.5.0 (McCune & Grace 2002).

Otolith growth indices

A subset of fish (n = 96) from 22 stations was selected for otolith increment analysis to as an indicator of *in situ* GRs. Stations were selected to be representative of the observed distribution of cod in the sampling area. Otoliths were dissected from the fish, rinsed, and stored dry prior to examination. From each pair, the right sagitta was embedded in resin (Polytranspar) and a transverse section that included the core was made using a low-speed, diamond-blade saw (Buhler IsoMet®). The section was polished (3M wetordry paper™ and lapping film) to reveal increment structure on the outer edge of the otolith's ventral margin. This region of the otolith section was photographed under magnification (400×), and image analysis software (Image-Pro Premier) was used to measure the widths of the outermost 20 to 30 clear increments. Given strong, positive relationships between body size (TL) and otolith size within all regions (r > 0.89 for all body–otolith size relationships), we considered otolith increment width a reasonable proxy for growth. Therefore, the mean width of the 20 outermost increments along the margin was used as an index of recent GR. We performed an additional analysis which took into account the differences in collection dates among specimens. The records of otolith increment widths were aligned chronologically based on increment counts relative to the capture date to estimate a GR over a fixed 10 d time window (5 to 15 Aug; GR_{sync}) for all sampled fish. Otolith GRs were analyzed across regions with 1-way ANOVA.

Bioenergetic analysis of growth potential

Bioenergetic models are mass balance equations representing the flow of energy within a fish from consumption to metabolism and growth (Hewett & Johnson 1992). For this analysis, we described spatial variation in growth potential across cod habitats in the SEBS applying the physiological model parameters developed for age-0 Pacific cod (see the Supplement at www.int-res.com/articles/suppl/m590p171_supp.pdf). Parameter estimation included fitting the allometry of consumption rate to published laboratory data on growth and respiration rates (Oh et al. 2010, Laurel et al. 2016). See the Supplement for details on model parameterization and parameter values.

Spatial variation in growth potential (GP_{cap}) was estimated across the SEBS based on water tempera-

tures observed during fish capture (T_{cap}) and station-specific prey ED_W. To account for the potential effect of differences in sampling date on observed temperature, we also estimated the temperature at each station from the model output from the PAROMS model of Bering Sea oceanography for 1 Sep 2012 and recalculated the growth potential based on these synchronous temperatures (GP_{2012}). The date of 1 Sep was used as it was in the middle of the field sampling interval, thereby requiring the minimum amount of temporal correction. For both estimates (GP_{cap} and GP_{2012}), ED_W of prey was calculated for each sampling station where cod were captured based on the diet composition observed at that station and ED_W estimates of specific prey groups (Table 2). At stations where no age-0 cod were captured (48%), ED_W of prey was assigned to the mean of other sampled stations in that region. The activity level (metabolic multiplier) was held constant across stations and regions. Potential GR at each station was estimated assuming maximum consumption rate ($P = 1$) for a 1.9 g cod with a mean ED_W of 4.138 kJ g^{-1} (observed overall mean).

We also performed a preliminary examination of interannual variation in the spatial pattern in habitat quality from a growth energetics perspective. For this analysis, we contrasted the estimates of growth potential obtained for 2012 (GP_{2012}, a cold year in the Bering Sea) with those estimated for 2005 (GP_{2005}) as a representative warm year in the Bering Sea (Stabeno et al. 2012). GP_{2005} was calculated for each station in the sampling region and was not dependent on the cod distribution observed in 2012. All inputs to the bioenergetic model were identical with the exception of station-specific temperatures and prey energy densities. Temperatures were obtained from the PAROMS model for 1 Sep 2005 based on the year-specific realization of the model. Temperatures were warmer in 2005 than in 2012 at 98% of the sampling locations, with an average difference of 1.7°C. The diet ED_W estimates for 2005 were estimated by applying the spatial pattern of diet ED_W observed in 2012, adjusting for the basin-wide differences in diet composition of age-0 cod observed between warm and cold years in the SEBS. Based on the multi-year analysis of diets presented in Farley et al. (2016), we calculated that mean ED_W of the diets averaged 3.14 kJ g^{-1} in warm years and 4.10 kJ g^{-1} in cold years. The ratio of these (0.832) was applied to the observed diet energy at each sampling station observed in 2012 to estimate station-specific diet energy values in 2005.

RESULTS

Size and energetic condition

The TL of age-0 Pacific cod varied among the sampling regions (K-W ANOVA, $H_6 = 354.7$, p < 0.001), but this pattern was primarily driven by the small sizes observed in the SL and KB regions (in pairwise post hoc tests, SL fish were smaller than fish in all other regions except KB; KB fish were smaller than fish in all other regions except SL and PMC, p < 0.05; Fig. 2). Fish in PMC were slightly, but not significantly smaller than the fish in regions AKP, BB, SM, and NM (all p > 0.10). There was no relationship between the mean fish size at a station and the temperature measured at the time of sampling (r = −0.194, p = 0.861, n = 84). We examined the effect of sampling date on the observed differences in body size by correcting observed lengths to a common date (1 Sep) using empirical region-specific GRs based on measurements of marginal otolith increments and the observed SL–otolith size relationships (regional r^2 = 0.763 to 0.910, n = 14 to 173). Correcting for differences in date of capture did not alter the observed regional pattern in TL variation (Fig. 2).

There was a significant effect of region on W_{dev} (K-W ANOVA, $H_6 = 30.3$, p < 0.001) due to the low values observed in PMC, which were significantly lower than values in all other regions (all pairwise p < 0.01; Fig. 2). Among the other regions, the highest mean value was observed in NM and lowest mean observed in AKP, but differences between regions were not significant (all remaining pairwise p > 0.30).

Due to the small number of fish captured in PMC, energy density measures were not available for this region. There was a weak, non-significant, positive correlation between ED_W and TL (r = 0.102, p = 0.316, n = 98). Fish from the BB and AKP regions had the highest and lowest energy levels, respectively, but the differences among regions were not significant (K-W ANOVA, $H_5 = 9.9$, p = 0.077). Across regions, there was a negative relationship between capture temperature and ED_W (r = −0.226, p = 0.025).

Stomach fullness and diet

Of 432 fish examined, only 2 had completely empty stomachs. Gut fullness across the sampling area averaged 2.2% of body weight (±1.5% SD). Despite high variation among fish, there was a weak, negative correlation between individual fish size and gut
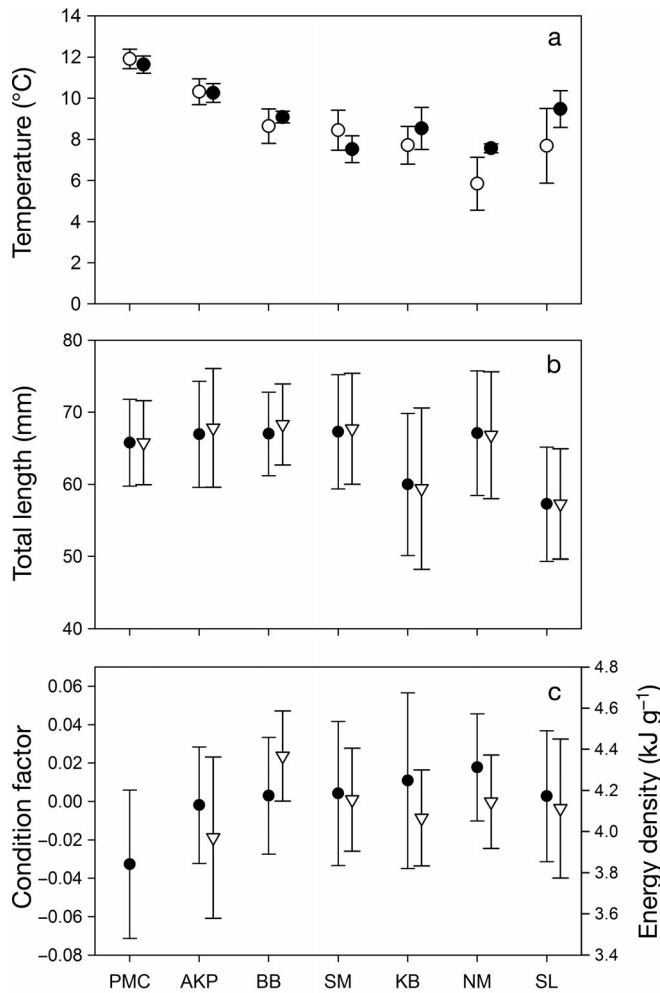
Fig. 2. Mean (±SD) water temperatures, total length, and energetic condition of age-0 Pacific cod in southeastern Bering Sea sampling regions. (a) Open circles: average temperatures measured at sampling locations; filled circles: weighted mean temperatures of capture (b) Circles: mean lengths measured at capture; triangles: lengths corrected to a common date of 1 Sep. (c) Circles: wet weight condition factors; triangles: energy density. See Fig. 1 for region abbreviations

fullness (correlations with body length and wet mass, $r < -0.17$, $p < 0.001$). Mean gut fullness varied across the sampling regions (K-W ANOVA of TL-adjusted values, $H_6 = 43.2$, $p < 0.001$; Table 3), with fullness in BB (3.6%) being significantly higher than in SM, SL, AKP, and PMC regions (all $p < 0.05$). Gut fullness was lowest in PMC (1.1%), significantly lower than that observed in all other regions ($p < 0.05$). Mean energy content of the diet was highest in AKP and BB (4.35 and 4.31 kJ g^{-1} respectively) and lowest in the SL region (3.74 kJ g^{-1}). Mean total stomach energy (calculated from gut fullness and prey energy density) was highest in BB (153.9 J g^{-1} fish weight) and lowest

in PMC (47.9 J g^{-1}), with all other regions averaging 81.2 to 98.0 J g^{-1}.

Throughout the SEBS, age-0 Pacific cod diets were primarily comprised of pelagic and hyperbenthic invertebrates but there were regional differences in primary prey types (Fig. 3). Euphausiids were a larger component of the diets in AKP and BB than other regions and pteropods were most important in SL. Amphipods and copepods were important diet items throughout the SEBS although the species consumed varied among regions. For amphipods, benthic species such as *Pacificulodes zernovi* were important in PMC and AKP with pelagic species including *Hyperoides longipes* being consumed in the deeper waters of SM. Similarly, hyperbenthic copepods such as *Eurytemora herdmandi* were consumed in the shallow waters of BB, AKP, and PMC in contrast to the pelagic species *Calanus marshallae* and *C. glacialis* consumed in SM, NM, and KB regions.

The patterns in diet composition among regions are reflected in the NMDS ordination of diets observed at each sampling station (Fig. 4). A 3-axis solution resulted in an ordination with final stress of 13.6% that accounted for 83% of the original multidimensional distance among stations. Axis 1 (explaining 45% of variation) was negatively correlated with water depth ($r = -0.756$) and longitude ($r = -0.663$) and positively correlated with temperature ($r = 0.492$), separating shallow stations where benthic copepods, amphipods, and cumaceans were abundant in the diet from offshore stations where crab larvae and pelagic copepods were more important. Axis 2 (explaining 18% of variation) further separated stations where euphausiids and benthic copepods were important from stations where pelagic copepods were important.

Growth rates

GR of age-0 Pacific cod in the SEBS were inferred from marginal otolith increment widths measured for 96 fish. GR over the 20 d prior to capture was not significantly correlated with body size (TL, $r = 0.189$, n = 90) or gut fullness ($r = -0.033$, $p = 0.763$). GR was positively correlated with water temperatures at the time of capture ($r = 0.232$, $p = 0.027$). The highest mean GRs were observed in AKP and PMC (Fig. 5) and lowest in KB, although there was no significant difference among sampling regions (K-W ANOVA, $H_6 = 10.0$, $p = 0.124$). GR$_{sync}$ was significantly correlated with GR ($r = 0.745$, $p < 0.001$), and reflected a similar regional pattern.

Table 3. Sample sizes, stomach fullness (±SD), energy density of diet components weighted by mass fraction, average stomach energy density, and diet composition of age-0 Pacific cod captured in the southeast Bering Sea, late summer 2012. Letters following prey types refer to benthic (b) or pelagic (p) species. %F = frequency of occurrence; %W = percent of total mass. See Fig. 1 for region abbreviations

|	— PMC —		— AKP —		— BB —		—SM—		—KB—		—NM —		— SL —	
Stomach fullness (% body weight)	1.13 (0.60)		2.25 (1.81)		3.57 (1.92)		2.06 (1.25)		2.03 (1.36)		2.07 (0.63)		2.45 (1.29)	
Diet energy density (kJ g^{-1} wet mass)	4.24		4.35		4.31		4.11		4.00		4.18		3.74	
Stomach energy (J prey g^{-1} fish)	47.9		98.0		153.9		84.6		81.2		86.6		91.6	
Prey type	%F	%W	%F	%W	%F	%W	%F	%W	%F	%W	%F	%W	%F	%W
Amphipods (b)	25.9	11.5	28.9	11.2	0	0	1.8	1.6	13.8	13.9	5.9	3.1	0	0
Amphipods (p)	7.4	5.5	7.8	7.5	66.7	15.4	44.6	20.2	6.9	1.5	29.4	4.9	61.9	18.1
Copepods (b)	77.8	45.2	64.1	17.2	3.7	0	0	0	3.4	0	0	0	0	0
Copepods (p)	11.1	0.4	13.3	0.3	25.9	1.8	66.1	34.6	75.9	28.3	88.2	61.6	52.4	19.5
Shrimps	7.4	0.3	0.8	0.1	59.3	17.5	41.1	14.5	41.4	15.4	41.2	25.2	28.6	13.4
Crabs	48.1	8.1	38.3	3.9	0	0	0.9	0.1	3.4	0	0	0	0	0
Cumaceans	0	0	47.7	34.4	74.1	49.9	30.4	18.5	13.8	9.5	5.9	5.2	28.6	18.3
Euphasiids	11.1	0.7	53.1	22.3	11.1	7.5	2.7	1.5	17.2	7.3	0	0	0	0
Mysids	0	0	0	0	0	0	16.1	7.4	17.2	7.6	0	0	42.9	18.2
Pteropods	14.8	8.9	13.3	1.3	11.1	1.3	1.8	0.1	34.5	16.0	0	0	4.8	1.0
Misc.	74.1	19.4	24.2	2.0	14.8	6.7	5.4	1.6	3.4	0.5	5.9	0.1	2.4	1.5
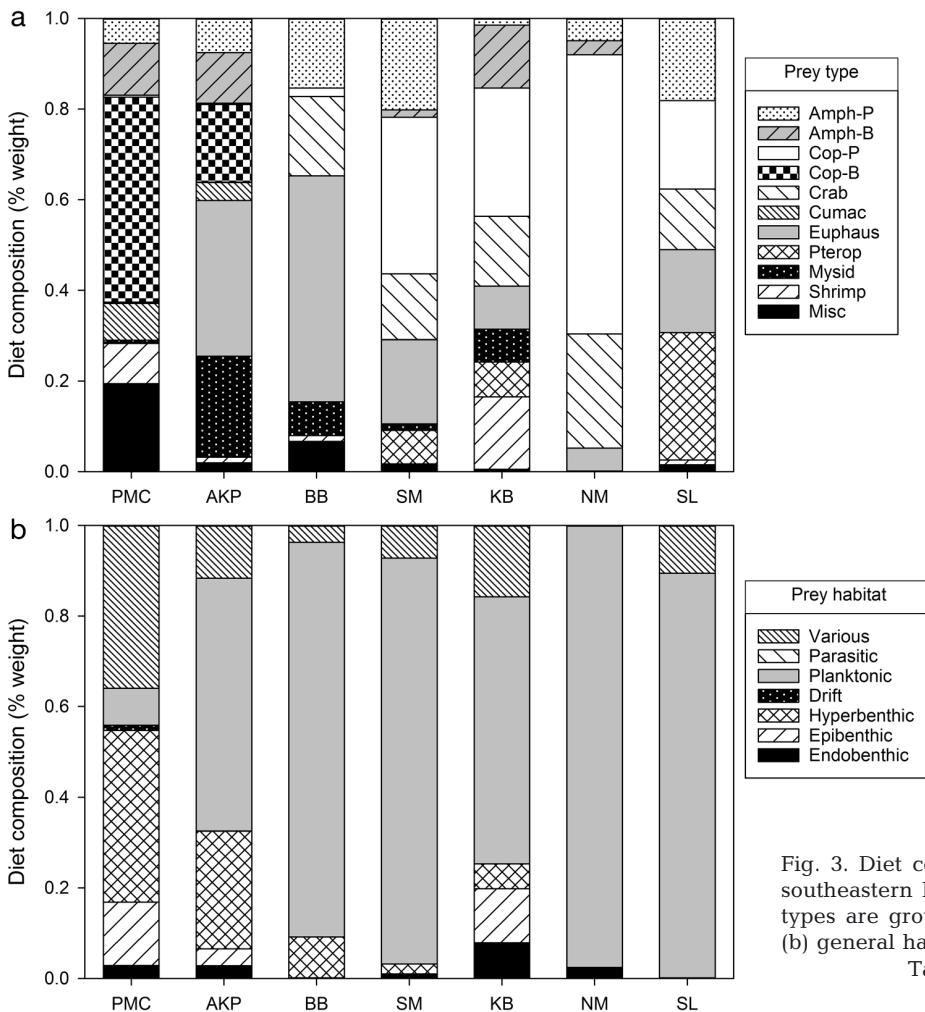
Fig. 3. Diet composition of age-0 Pacific cod in southeastern Bering Sea sampling regions. Prey types are grouped into (a) major prey taxa and (b) general habitat classifications. See Fig. 1 and Table 3 for abbreviations

Bioenergetic models

Cod GP_{cap} estimated for each sampling station ranged from 1.59 to 4.47% d^{-1}. GP_{cap} was positively correlated with mean observed GR (otolith increment width) measured at that station (r = 0.449, p = 0.036, n = 22). In addition, modeled GRs were positively correlated with observed energy density of fish at each station (r = 0.361, p = 0.010, n = 50), further suggesting that the bioenergetic model accurately captured the spatial patterns in the growth environment of age-0 cod in the Bering Sea.

To account for spatial differences in the timing of field sampling, we estimated GP_{2012} using the bioenergetic model for a standardized date of 1 Sep using temperature output from the PAROMS model. The resulting estimates of growth potential were less variable than the estimates based on the temperatures measured during field sampling (ratio of max./min. GP_{2012} 2.02 vs. 2.81 for GP_{cap}). Average GP_{2012} across the sampling regions was 3.55% d^{-1}. The lowest estimated growth potential (2.27% d^{-1}) observed at a station in the KB region was approximately half that of the highest rate (4.58% d^{-1}) observed in the AKP region (Fig. 6). Averaging across stations in each region, the highest mean GP_{2012} (3.99% d^{-1}) was observed in AKP followed by BB (3.81% d^{-1}). The lowest mean GP_{2012} were observed in the KB (3.44% d^{-1}) and SL regions (3.18% d^{-1}).

We examined the effects of basin-wide climate conditions for cod growth in the SEBS by parameterizing the growth model for 2005, a representative warm year. We applied the temperature field from the 2005 realization of the PAROMS model and adjusted the prey energy density for observed differences between warm and cold climate regimes. The combined changes resulted in GP_{2005} estimates that were, on average, 20% lower than the GP_{2012} values. In addition, there was a change in the region with the highest growth potential from AKP (in 2012) to BB (in 2005). The SL region had the lowest growth potentials in both years. While the reduced prey energy density negatively affected GP_{2005} throughout the basin, the degree of growth reduction varied among regions depending on the thermal conditions. GP in PMC and AKP was >25% lower in 2005 than in 2012 as GP_{2005} in those re-
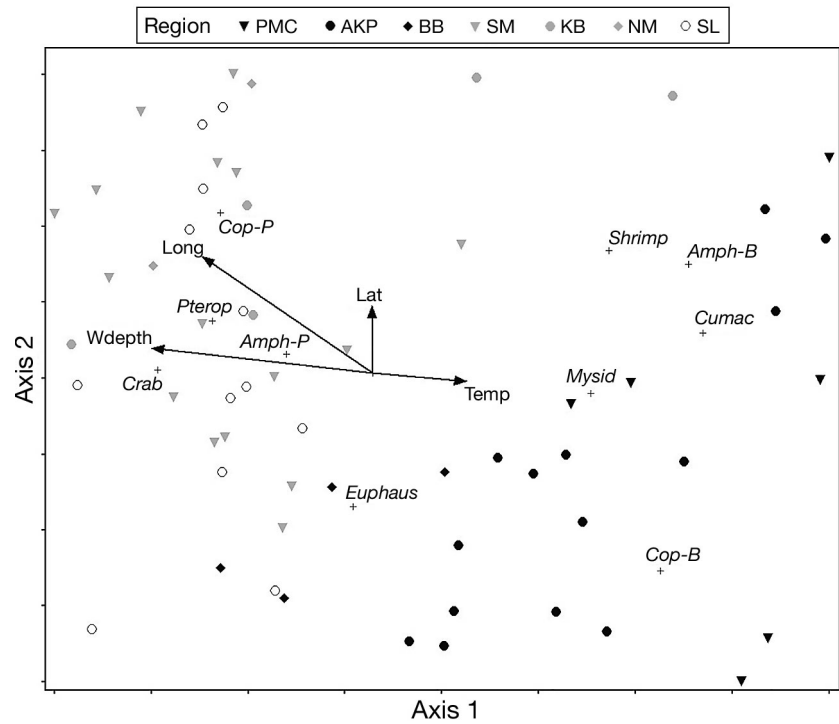

Fig. 4. Non-metric multi-dimensional scaling of station-specific diet composition of age-0 Pacific cod in the south-eastern Bering Sea. See Fig. 1 and Table 3 for abbreviations
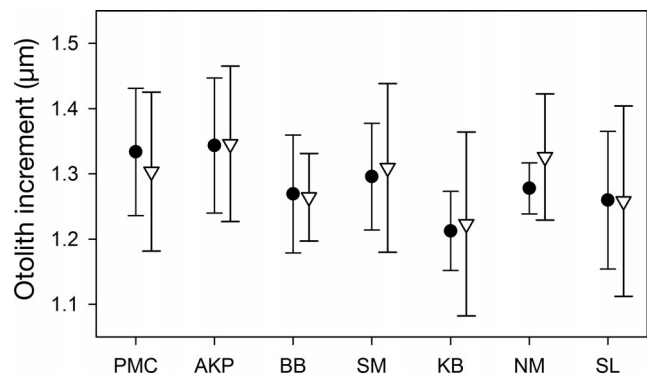

Fig. 5. Mean (±SD) growth rates of age-0 Pacific cod inferred from widths of otolith increments. ●: regional means of most recent 20 increments deposited prior to capture; ∇: mean of increments deposited during 5 to 15 Aug 2012. See Fig. 1 for region abbreviations

gions was further reduced by temperatures that exceeded the maximum for growth (11.6°C). Conversely, the difference in GP between years was lowest in KB, where the increase in maximum consumption associated with warmer temperatures in 2005 partially offset the effects of reduced prey energy density. As a result, GP in the KB region was only 10% lower in 2005 than 2012.
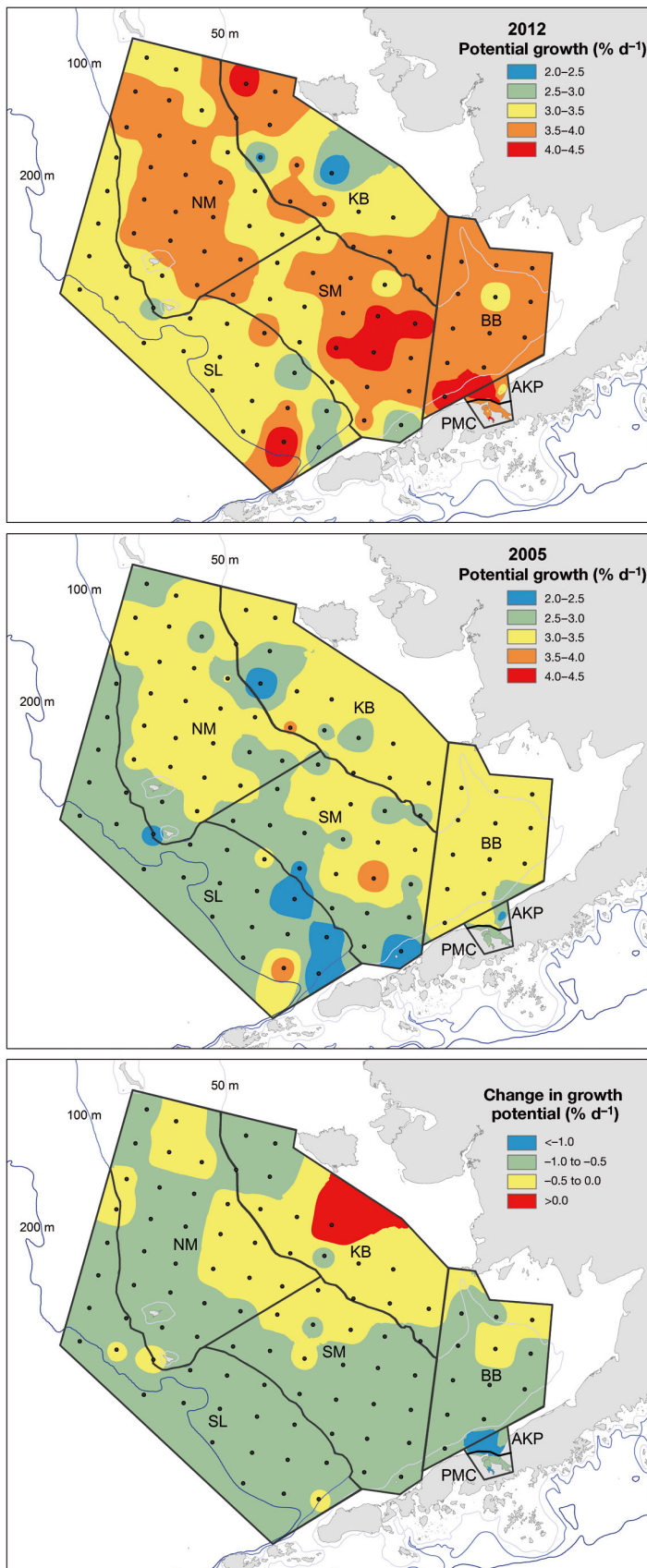
Fig. 6. Growth potential of age-0 Pacific cod in (a) late summer 2012 and (b) 2005; (c) difference in growth potential between the cold year of 2012 and the warm year of 2005. Growth potential is based on estimates of temperature and prey energy density for each sampling station. Closely spaced sampling stations in the AKP and PMC region are not shown on the map. See Fig. 1 for region abbreviations

DISCUSSION

The distribution of early life stages of fishes can have a significant impact on the thermal conditions and prey field that they encounter, which are 2 key factors that drive growth, survival, and recruitment. Recent work has greatly expanded our understanding of the habitat use of age-0 cod in the SEBS, pointing to the primary use of 2 distinct habitat types: surface waters over the wide continental shelf and demersal areas along the central Alaska Peninsula (Hurst et al. 2012, 2015, Parker-Stetter et al. 2013). These habitats likely offer different conditions for foraging, growth, and survival. Here, we described regional spatial variation in growth energetics of juvenile cod through diet composition, energy density, and growth rates. These data were used to parameterize a spatially explicit bioenergetic model of growth potential of age-0 cod in the SEBS. The growth potential predicted by the model was correlated with observed otolith growth rates, providing strong support for the robustness of the model. Applying the bioenergetic model to a representative warm year demonstrated that climate conditions reduced the basin-wide mean growth potential and resulted in a shift in location of areas offering highest growth potential. Based on these observations we hypothesize that cod recruitment in the Bering Sea is linked to the spatial dynamics of habitat use and climate-driven prey field variation, responses which have been observed in other gadid populations (Kristiansen et al. 2014, Lough et al. 2017).

Diet variation

Several previous studies have examined the diets of age-0 gadids in the Bering Sea (e.g. Moss et al. 2009, Siddon et al. 2013, Strasburger et al. 2014, Farley et al. 2016),

but these focused primarily on the pelagic habitats over the middle and outer shelf. Here, we provide comparative information for the previously un-sampled nearshore habitats of PMC and AKC and supplement the under-sampled BB and KB regions. Across the sampling area, the diets we observed for cod in 2012 were generally similar to those observed in other cold years (Strasburger et al. 2014, Farley et al. 2016). Euphausiids were the largest single component of the diet in both previous studies, with copepods, crab (zoea and megalopae), and amphipods also being important. These prey types were observed in 2012 in varying amounts in different regions. Strasburger et al. (2014) noted a higher abundance of arrow worms *Parasagitta elegans* in a small sample of fish in 2010 (another cold year). However, these were found in <1% of cod stomachs collected in 2012.

The regional patterns in diet of age-0 cod reflect some expected patterns in the available prey fields. In shallower areas along the Alaska Peninsula and in Kuskokwim Bay, cod diets included more benthic and epibenthic prey such as shrimps and benthic species of amphipods and copepods. Conversely, over the deeper areas of the shelf, cod diets were dominated by pelagic species of copepods and amphipods as well as crab larvae. Previous studies documented the occurrence of pteropods as a minor component of the diets of both cod and walleye pollock (Moss et al. 2009, Strasburger et al. 2014, Farley et al. 2016). Our analysis suggested a strong degree of spatial variation in consumption of this prey type, with pteropods being most important (>20% by weight) in diets of cod caught in the SL region. Although focused on larger fish, a multi-year summary of walleye pollock diets observed some similar regional patterns to those observed in age-0 cod: mysids and other shrimp species were more abundant in the diets of small (<20 cm) walleye pollock over the inner shelf, whereas copepods dominated the diets in the deeper waters over the shelf and slope (Buckley et al. 2016).

Growth and condition

Empirical evaluations of habitat 'quality' are frequently based on spatial variation in physiological parameters such as energetic content or growth rate. This is based on the recognition that both aspects of energetics have direct linkages to survival. Whereas rapid growth reduces the potential for size-selective predation, increased energy stores minimize the risk

of starvation mortality. The seasonal and ontogenetic patterns of the allocation of energy between growth and lipid storage have been examined in a range of fish species (Post & Parkinson 2001, Hurst & Conover 2003, Siddon et al. 2013). Broadly speaking, energy is allocated primarily to somatic growth at small body sizes (when risk of predation mortality is high), with allocation shifting to storage as body size increases (risk of predation decreases). For fishes in temperate and boreal habitats, winter represents an energetically stressful period of reduced prey availability and metabolic expenditures exceeding energy intake through feeding (Hurst 2007). The potential for winter starvation appears to be responsible for the commonly observed seasonal cycle of lipid storage increasing in the late summer and autumn, prior to winter (Schultz & Conover 1997, Lea et al. 2015, but see Copeman et al. 2008).

In this study, we examined metrics of both growth and energy storage, and it is interesting to note that they offered differing perspectives on spatial variation in habitat quality. Fish from the AKP region exhibited the highest growth rates, but had the lowest energy density (of the regions measured). Because of the small numbers of fish captured in PMC, we were unable to obtain energy density estimates for this region. However, the very low condition factors observed in the region would suggest low energy densities in PMC, despite fish having high growth rates. These regions are contrasted with BB, where cod had very high energy densities, but only moderate growth rates.

The explanation for the apparent regional differences in growth-storage allocation of available energy is not known, but may be related to some aspects of the environment. Although both BB and AKP are relatively warm with high prey energy density, BB is slightly cooler with higher prey energy density than AKP. It is interesting to note that these spatial differences in cod energy density observed in 2012 appear to reflect the interannual differences observed by Farley et al. (2016) in age-0 SEBS cod. In warm years, cod consumed lower-energy prey (primarily walleye pollock and crab zoea) than in cold years when cod consumed more euphausiids, copepods, and amphipods (as observed here). As a result of these diet differences or the associated temperature differences (Copeman et al. 2017), cod in warm years were larger in size, but had lower energy storage levels than in cold years. Further work examining the potential environmental regulators of the energy allocation strategies of juvenile cod would clarify how expected climate variation would be pre-

dicted to impact the energetics of overwinter survival in this species.

Bioenergetic model growth estimates

Bioenergetic models offer a powerful tool to integrate information on aspects of the environment to describe the 'value' of a habitat from an energetics perspective. As in other applications of this tool, the model for age-0 cod was based upon a suite of independent laboratory experiments to derive temperature- and size-dependent functions for metabolism, consumption, and growth rate (M. Zaleski et al. unpubl. data). While this model has been applied in habitat analysis in the Gulf of Alaska (M. Zaleski et al. unpubl. data), it had previously not been validated with independent growth information. The correlation observed here between model predictions of growth potential and independent, empirical estimates of growth rates from otolith increment analysis provide a robust validation of the model for age-0 cod.

One aspect of bioenergetic models that has come under routine scrutiny is the estimation of activity costs (usually incorporated as a multiplier of 'routine' or 'basal' metabolism; Brodie et al. 2016). It is possible that cod in the 2 distinct habitat types examined here (shelf–surface vs. coastal–demersal) could exhibit different levels of activity that are not accounted for in the model (Madenjian et al. 2012). However, without specific information of how the activity levels differ, we did not vary activity costs across the habitats. The correlation between model-predicted and observed growth (from otolith increments) suggests that any such habitat-specific differences in activity, if they exist, did not overly impact model predictions of growth potential.

The analysis of habitat quality across broad geographic areas such as the Bering Sea can be complicated by the inability to synchronously sample across the area of interest. As a result, changing conditions during the sampling interval can potentially lead to misrepresentation of temporal variation as spatial variation. In surveys of the Bering Sea shelf, samples are generally collected working from the southeast to the northwest, such that the location and timing of sampling are linked. To account for this effect, we used the temperatures derived for a standardized date from an oceanographic model of the SEBS to estimate growth potential of cod. Correcting for the temporal pattern in sampling temperatures (by applying synchronous temperature estimates from the PAROMS model) reduced the perceived spatial variation in growth potential (ratio of max./min. across stations) by 28%.

Habitat use and recruitment of cod

While several cod populations are known to occupy multiple habitat types during the first year of life, previous analyses of the interactions between temperature, prey field, growth, and survival have generally focused exclusively on the coastal (e.g. Laurel et al. 2017) or offshore pelagic habitats (e.g. Eriksen et al. 2012, Lough et al. 2017). The relationship between the distribution of fish across habitat types and the spatial and interannual variation of growth potential in each habitat could be an important driver of recruitment as climate conditions vary (Siddon et al. 2013, Stige et al. 2015). Age-0 Pacific cod in the SEBS appear to exhibit habitat selection in response to these variable growth conditions. Hurst et al. (2012) showed that within sampling regions, age-0 cod were more abundant at warmer stations. While bioenergetic model estimates of GP did not vary between occupied and unoccupied stations in the AKP and PMC regions (Fig. 7), in pelagic habitats over the shelf, the growth potential was consistently higher at stations where cod were captured than stations where cod were absent. This difference was greatest in the NM and SL regions where, respectively, the estimated growth potential was 23 and 17% greater at occupied than at unoccupied stations in the same region.

At the larger, basin scale, cod distribution appears to generally match the distribution of areas offering the greatest opportunities for growth, but climate variation may disrupt that association. Age-0 cod are consistently more abundant in the warmer, southern regions of the SEBS (Hurst et al. 2012, 2015). Because temperature has a direct effect on the growth potential of cod, this would be expected to translate into higher growth potential unless temperatures exceed the maximum temperature for growth or prey are insufficient in those higher-temperature habitats. These analyses confirmed those predictions by specifically accounting for spatial variation in diet composition. The shallow waters along the Alaska Peninsula supported markedly higher (>10×) densities of cod (Hurst et al. 2015) and offered greater growth potential (in the 2012 sampling year) than offshore pelagic habitats.

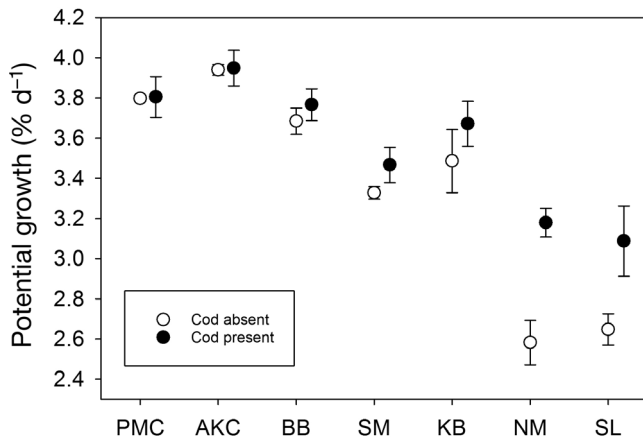However, it is unclear how the population may respond to basin-wide declines in growth potential

Fig. 7. Mean (±SE) estimated growth rate potential of age-0 Pacific cod in sampling regions of the southeastern Bering Sea. Points are the mean of station estimates within each region (see Fig. 1 for region abbreviations). Growth rates at stations where fish were caught are estimated using station-specific water temperature and prey energy density. For un-occupied stations, estimates are based on station-specific temperatures and the observed regional mean prey energy density

and shifts in the spatial distribution of 'optimal' habitat caused by climate variation. Lacking multiple years of broad, spatially explicit diet information, we limited our analysis of interannual variation in GP to illustrating 2 primary forcing mechanisms and their likely regional and basin-wide impacts. Estimated growth potential in the warm year of 2005 was lower than that in the cold year of 2012 in all sampling regions. The biggest reductions were observed in the southern, coastal regions of PMC and AKP which had temperatures near the thermal optimum for growth in cool climate conditions, such that growth rates were negatively impacted by both the temperature and prey field changes in warmer years. It is important to recognize that the 2 regions supporting the highest densities of age-0 cod (AKP and SM; Hurst et al. 2015) exhibited the largest declines in growth potential between cold and warm years (27 and 16%, respectively). Given the hypothesized link between summer growth and winter survival and recruitment of cod, this basin-wide reduction in growth potential could indicate declining habitat quality in a warming SEBS.

Associated with the overall decline in growth potential was a shift in the region that offered the highest growth potential (from AKP to BB). The potential impact of basin-wide declines in GP would be partially mitigated if age-0 cod exhibited a distributional shift that maintained the highest densities in the most favorable habitats. However,

there is little evidence that such shifts occur in juvenile cod (Eriksen et al. 2012, Hurst et al. 2012). Together, these findings suggest the potential for a climate-mediated mismatch of juvenile Pacific cod and the habitats offering the maximum growth potential, similar to that proposed for walleye pollock in the SEBS (Siddon et al. 2013) and Atlantic cod on Georges Bank (Lough et al. 2017). Given the importance of the Pacific cod fishery, additional research should further examine the potential for warming conditions to negatively affect juvenile cod growth and recruitment in the SEBS. This would entail better understanding of the variation in the prey field and diets of cod in the nearshore habitats as well as identifying the biological and oceanographic factors responsible for the basin-wide distribution of juveniles.

Conclusion

The recruitment and population productivity of resource species are driven by the distribution of individuals across the available habitats and the vital rates of growth and survival in those habitats. This work showed that nearshore habitats supporting the highest densities of age-0 cod offered the greatest growth potential in the cold sampling year. The spatial coincidence of high density and growth potential would be expected to result in high survival of the cohort. However, the impacts of climate change on fishery populations will be influenced by how thermal changes affect the productivity of nursery habitats as well as the extent to which fish distribution can track spatial changes in the location of optimal habitats. The northward shifts observed among some temperate fishery species may be associated with shifting locations of the optimal nursery habitats (Perry et al. 2005). In the SEBS, our bioenergetic model estimates indicated temporal shifts in the region(s) offering the greatest growth potential. Combined with observations of distributional stability in the face of thermal variation, these patterns suggest the potential for climate-induced spatial mismatch in this and other cod populations (Eriksen et al. 2012, Hurst et al. 2012, Lough et al. 2017). Conversely, a persistent change in habitat quality resulting in juvenile Pacific cod shifting from coastal to pelagic habitats over the SEBS shelf would lead to increased overlap with age-0 walleye pollock, which may have important implications for the recruitment of both species.

LITERATURE CITED

Abookire AA, Duffy-Anderson JT, Jump CM (2007) Habitat associations and diet of young-of-the-year Pacific cod (*Gadus macrocephalus*) near Kodiak, Alaska. Mar Biol 150:713–726

Anderson JT, Dalley EL (1997) Spawning and year-class strength of northern cod (*Gadus morhua*) as measured by pelagic juvenile cod surveys, 1991-1994. Can J Fish Aquat Sci 54:158–167

Beaugrand G, Kirby RR (2010) Climate, plankton and cod. Glob Change Biol 16:1268–1280

Benjamin JR, Connolly PJ, Romine JG, Perry R (2013) Potential effects of changes in temperature and food resources on life history trajectories of juvenile *Oncorhynchus mykiss.* Trans Am Fish Soc 142:208–220

Bergstad OA, Jorgensen T, Dragesund O (1987) Life-history and ecology of the gadoid resources of the Barents Sea. Fish Res 5:119–161

Brodie S, Taylor MD, Smith JA, Suthers IM, Gray CA, Payne NL (2016) Improving consumption rate estimates by incorporating wild activity into a bioenergetics model. Ecol Evol 6:2262–2274

Buckley TW, Ortiz I, Aydin K (2016) Summer diet composition of walleye pollock and predator–prey relationships with copepods and euphausiids in the eastern Bering Sea, 1987-2011. Deep Sea Res II 134:302–311

Cooper DW, Duffy-Anderson JT, Norcross BL, Holladay BA, Stabeno PJ (2014) Northern rock sole (*Lepidopsetta polyxystra*) juvenile nursery areas in the eastern Bering Sea in relation to hydrography and thermal regimes. ICES J Mar Sci 71:1683–1695

Copeman LA, Parrish CC, Gregory RS, Wells JS (2008) Decreased lipid storage in juvenile Atlantic cod (*Gadus morhua*) during settlement in cold-water eelgrass habitat. Mar Biol 154:823–832

Copeman LA, Laurel BJ, Spencer M, Sremba A (2017) Temperature impacts on lipid allocation among juvenile gadid species at the Pacific Arctic-Boreal interface: an experimental laboratory approach. Mar Ecol Prog Ser 566:183–198

Coyle KO, Eisner LB, Mueter FJ, Pinchuk AI and others (2011) Climate change in the southeastern Bering Sea: impacts on pollock stocks and implications for the oscillating control hypothesis. Fish Oceanogr 20:139–156

Dalley EL, Anderson JT (1997) Age-dependent distribution of demersal juvenile Atlantic cod (*Gadus morhua*) in inshore/offshore northeast Newfoundland. Can J Fish Aquat Sci 54:168–176

Davis KW, Myers KW, Ishida A (1998) Caloric value of high-seas salmon prey organisms and simulated salmon ocean growth and prey consumption. N Pac Anadr Fish Comm Bull 1:146–162

Eriksen E, Ingvaldsen R, Stiansen JE, Johansen GO (2012) Thermal habitat for 0-group fish in the Barents Sea; how climate variability impacts their density, length, and geographic distribution. ICES J Mar Sci 69:870–879

Farley EV Jr, Murphy JM, Adkison MD, Eisner LB, Helle JH, Moss JH, Nielsen J (2007) Early marine growth in relation to marine-stage survival rates for Alaska sockeye salmon (*Oncorhynchus nerka*). Fish Bull 105:121–130

Farley EV, Heintz RA, Andrews AG, Hurst TP (2016) Size, diet, and condition of age-0 Pacific cod (*Gadus macrocephalus*) during warm and cool climate states in the eastern Bering Sea. Deep Sea Res II 134:247–254

Heintz RA, Siddon EC, Farley EV, Napp JM (2013) Correlation between recruitment and fall condition of age-0 pollock (*Theragra chalcogramma*) from the eastern Bering Sea under varying climate conditions. Deep Sea Res II 94:150–156

Hewett SW, Johnson BL (1992) Fish bioenergetics model 2: an upgrade of 'A generalized bioenergetics model of fish growth for microcomputers'. University of Wisconsin Sea Grant Technical Report WIS-SG-92-250, University of Wisconsin, Madison, WI

Houde ED (1987) Fish early life dynamics and recruitment variability. Am Fish Soc Symp 2:17–29

Hurst TP (2007) Causes and consequences of winter mortality in fishes. J Fish Biol 71:315–345

Hurst TP, Conover DO (2003) Seasonal and interannual variation in the allometry of energy allocation in juvenile striped bass. Ecology 84:3360–3369

Hurst TP, Moss JH, Miller JA (2012) Distributional patterns of 0-group Pacific cod (*Gadus macrocephalus*) in the eastern Bering Sea under variable recruitment and thermal conditions. ICES J Mar Sci 69:163–174

Hurst TP, Cooper DW, Duffey-Anderson JT, Farley EV (2015) Contrasting coastal and shelf nursery habitats of Pacific cod in the southeastern Bering Sea. ICES J Mar Sci 72:515–527

Kinder TH, Schumacher JD (1981) Hydrographic structure over the continental shelf of the southeastern Bering Sea. In: Hood DW, Calder JA (eds) The eastern Bering Sea shelf: oceanography and resources. University of Washington Press, Seattle, WA, p 31–52

Kristiansen T, Stock C, Drinkwater KF, Curchitser EN (2014) Mechanistic insights into the effects of climate change on larval cod. Glob Change Biol 20:1559–1584

Laurel BJ, Stoner AW, Ryer CH, Hurst TP, Abookire AA (2007) Comparative habitat associations in juvenile Pacific cod and other gadids using seines, baited cameras and laboratory techniques. J Exp Mar Biol Ecol 351: 42–55

Laurel BJ, Spencer M, Iseri P, Copeman LA (2016) Temperature-dependent growth and behavior of juvenile Arctic cod (*Boreogadus saida*) and co-occurring North Pacific gadids. Polar Biol 39:1127–1135

Laurel BJ, Cote D, Gregory RS, Rogers L, Knutsen H, Olsen EM (2017) Recruitment signals in juvenile cod surveys depend on thermal growth conditions. Can J Fish Aquat Sci 74:511–523

Lea EV, Mee JA, Post JR, Rogers SM, Mogensen S (2015) Rainbow trout in seasonal environments: phenotypic trade-offs across a gradient in winter duration. Ecol Evol 5:4778–4794

Lough RG, Broughton EZ, Kristiansen T (2017) Changes in spatial and temporal variability of prey affect functional connectivity of larval and juvenile cod. ICES J Mar Sci 74:1826–1837

Madenjian CP, David SR, Pothoven SA (2012) Effects of activity and energy budget balancing algorithm on laboratory performance of a fish bioenergetics model. Trans Am Fish Soc 141:1328–1337

Marin Jarrin J (2012) Sandy beach surf zones: What is their role in the early life history of Chinook salmon? PhD dissertation, Oregon State University, Corvallis, OR

McCune B, Grace JB (2002) Analysis of ecological communities. MjM Software Design, Gleneden Beach, OR

Miller JA, DiMaria RA, Hurst TP (2016) Patterns of larval source distribution and mixing in early life stages of Pacific cod (*Gadus macrocephalus*) in the southeastern Bering Sea. Deep Sea Res II 134:270–282

Moss JH, Farley EV, Feldmann AM, Ianelli JN (2009) Spatial distribution, energetic status, and food habits of eastern Bering Sea age-0 walleye pollock. Trans Am Fish Soc 138:497–505

Mueter FJ, Boldt JL, Megrey BA, Peterman RM (2007) Recruitment and survival of Northeast Pacific Ocean fish stocks: temporal trends, covariation, and regime shifts. Can J Fish Aquat Sci 64:911–927

Nishiyama T (1977) Food-energy requirements of Bristol Bay sockeye salmon *Oncorhynchus nerka* (Walbaum) during the last marine life stage. Res Inst North Pacific Fish Spec Vol, p 289–320. Hokkaido University, Hokodate

Oh SY, Park HS, Kim CK (2010) Effect of water temperature and photoperiod on the oxygen consumption rate of juvenile Pacific cod *Gadus macrocephalus.* Ocean Polar Res 32:229–236

Ortiz I, Aydin K, Hermann AJ, Gibson GA and others (2016) Climate to fish: synthesizing field work, data and models in a 39-year retrospective analysis of seasonal processes on the eastern Bering Sea shelf and slope. Deep Sea Res II 134:390–412

Overland JE, Salo SA, Kantha LH, Clayson CA (1999) Thermal stratification and mixing on the Bering Sea Shelf. In: Loughlin TR, Ohtani K (eds) Dynamics of the Bering Sea. University of Alaska Sea Grant, Fairbanks, AK

Parker-Stetter SL, Horne JK, Farley EV, Barbee DH, Andrews AG, Eisner L, Cieciel KD (2013) Summer distributions of forage fish in the eastern Bering Sea. Deep Sea Res II 94:211–230

Perez MA (1990) Review of marine mammal population and prey information for Bering Sea ecosystem studies. NOAA Technical Memo NMFS-F/NWC-186. National Marine Mammal Laboratory, Seattle, WA

Perry AL, Low PJ, Ellis JR, Reynolds JD (2005) Climate change and distributional shifts in marine fishes. Science 308:1912–1915

Pörtner HO, Peck MA (2010) Climate change effects on fishes and fisheries: towards a cause-and-effect understanding. J Fish Biol 77:1745–1779

Post JR, Parkinson EA (2001) Energy allocation strategy in young fish: allometry and survival. Ecology 82:1040–1051

Salvanes AGV, Skjaeraasen JE, Nilsen T (2004) Sub-populations of coastal cod with different behaviour and life-history strategies. Mar Ecol Prog Ser 267:241–251

Schultz ET, Conover DO (1997) Latitudinal differences in somatic energy storage: adaptive responses to seasonality in an estuarine fish (Atherinidae: *Menidia menidia*). Oecologia 109:516–529

Shchepetkin AF, McWilliams JC (2005) The regional oceanic modeling system (ROMS): a split-explicit, free-surface, topography-following-coordinate oceanic model. Ocean Model 9:347–404

Siddon EC, Heintz RA, Mueter FJ (2013) Conceptual model of energy allocation in walleye pollock (*Theragra chalcogramma*) from age-0 to age-1 in the southeastern Bering Sea. Deep Sea Res II 94:140–149

Sigler MF, Napp JM, Stabeno PJ, Heintz RA, Lomas MW, Hunt GL (2016) Variation in annual production of copepods, euphausiids, and juvenile walleye pollock in the southeastern Bering Sea. Deep Sea Res II 134:223–234

Stabeno PJ, Kachel NB, Moore SE, Napp JM, Sigler M, Yamaguchi A, Zerbini AN (2012) Comparison of warm and cold years on the southeastern Bering Sea shelf and some implications for the ecosystem. Deep Sea Res II 65–70:31–45

Stige LC, Langangen O, Yaragina NA, Vikebo FB and others (2015) Combined statistical and mechanistic modelling suggests food and temperature effects on survival of early life stages of Northeast Arctic cod (*Gadus morhua*). Prog Oceanogr 134:138–151

Strasburger WW, Hillgruber N, Pinchuk AI, Mueter FJ (2014) Feeding ecology of age-0 walleye pollock (*Gadus chalcogrammus*) and Pacific cod (*Gadus macrocephalus*) in the southeastern Bering Sea. Deep Sea Res II 109:172–180

Sundby S (2000) Recruitment of Atlantic cod stocks in relation to temperature and advection of copepod populations. Sarsia 85:277–298

Whitman LD (2010) Variation in the energy density of forage fishes and invertebrates from the southeast Bering Sea. MSc thesis, Oregon State University, Corvallis, OR

Wilt LM (2012) Caloric content of Bering and Chuckchi Sea benthic invertebrates. MSc thesis, University of Maryland, College Park, MD